




Cyclic AMP-Independent Control of Twitching Motility in *Pseudomonas aeruginosa*

Ryan N. C. Buensuceso,^a Martin Daniel-Ivad,^b Sara L. N. Kilmury,^a
Tiffany L. Leighton,^a Hanjeong Harvey,^a P. Lynne Howell,^{b,c}  Lori L. Burrows^a

Department of Biochemistry and Biomedical Sciences and Michael G. DeGroote Institute for Infectious Disease Research, McMaster University, Hamilton, Ontario, Canada^a; Program in Molecular Medicine, The Hospital for Sick Children, Toronto, Ontario, Canada^b; Department of Biochemistry, University of Toronto, Toronto, Ontario, Canada^c

ABSTRACT FimV is a *Pseudomonas aeruginosa* inner membrane hub protein that modulates levels of the second messenger, cyclic AMP (cAMP), through the activation of adenylate cyclase CyaB. Although type IVa pilus (T4aP)-dependent twitching motility is modulated by cAMP levels, mutants lacking FimV are twitching impaired, even when exogenous cAMP is provided. Here we further define FimV's cAMP-dependent and -independent regulation of twitching. We confirmed that the response regulator of the T4aP-associated Chp chemotaxis system, PilG, requires both FimV and the CyaB regulator, FimL, to activate CyaB. However, in cAMP-replete backgrounds—lacking the cAMP phosphodiesterase CpdA or the CheY-like protein PilH or expressing constitutively active CyaB—*pilG* and *fimV* mutants failed to twitch. Both cytoplasmic and periplasmic domains of FimV were important for its cAMP-dependent and -independent roles, while its septal peptidoglycan-targeting LysM motif was required only for twitching motility. Polar localization of the sensor kinase PilS, a key regulator of transcription of the major pilin, was FimV dependent. However, unlike its homologues in other species that localize flagellar system components, FimV was not required for swimming motility. These data provide further evidence to support FimV's role as a key hub protein that coordinates the polar localization and function of multiple structural and regulatory proteins involved in *P. aeruginosa* twitching motility.

IMPORTANCE *Pseudomonas aeruginosa* is a serious opportunistic pathogen. Type IVa pili (T4aP) are important for its virulence, because they mediate dissemination and invasion via twitching motility and are involved in surface sensing, which modulates pathogenicity via changes in cAMP levels. Here we show that the hub protein FimV and the response regulator of the Chp system, PilG, regulate twitching independently of their roles in the modulation of cAMP synthesis. These functions do not require the putative scaffold protein FimL, proposed to link PilG with FimV. PilG may regulate asymmetric functioning of the T4aP system to allow for directional movement, while FimV appears to localize both structural and regulatory elements—including the PilSR two-component system—to cell poles for optimal function.

KEYWORDS *Pseudomonas aeruginosa*, subcellular localization, twitching motility, type IV pili

Type IV pili (T4P) are polar filamentous surface appendages made by a broad range of bacteria and archaea (1, 2). They can be divided into two subfamilies, type IVa pili (T4aP) and T4bP, which—though clearly related—differ in their pilin subunits and assembly system architectures (2). T4aP are involved in several processes, including

Received 15 March 2017 Accepted 23 May 2017

Accepted manuscript posted online 5 June 2017

Citation Buensuceso RNC, Daniel-Ivad M, Kilmury SLN, Leighton TL, Harvey H, Howell PL, Burrows LL. 2017. Cyclic AMP-independent control of twitching motility in *Pseudomonas aeruginosa*. J Bacteriol 199:e00188-17. <https://doi.org/10.1128/JB.00188-17>.

Editor George O'Toole, Geisel School of Medicine at Dartmouth

Copyright © 2017 American Society for Microbiology. All Rights Reserved.

Address correspondence to P. Lynne Howell, howell@sickkids.ca, or Lori L. Burrows, burrowl@mcmaster.ca.

DNA uptake, surface attachment, and twitching motility (3–5). During twitching motility, T4aP undergo repeated cycles of assembly and disassembly, acting as molecular grappling hooks to pull the cells along surfaces. Well-studied T4aP model species include *Neisseria* spp., *Myxococcus xanthus*, and *Pseudomonas aeruginosa* (6, 7). Although core structural components of the T4aP assembly machinery and pilus fiber are shared, each species has unique regulatory elements that control the function of the T4aP machinery in response to their specific environmental requirements. Without these regulatory proteins, the bacteria make nonfunctional T4aP systems (8–11).

The *P. aeruginosa* Chp system is a putative chemosensory system that controls both twitching motility and intracellular levels of the second messenger, cyclic AMP (cAMP) (12–14). It resembles the well-studied Che system of *Escherichia coli* but lacks a CheZ-like phosphatase. Rather, similar to *Sinorhizobium meliloti* (15), it has two CheY-like response regulators, PilG and PilH (14, 16). PilG is proposed to regulate the activation of CyaB and pilus extension (17), while PilH has been proposed to be either a phosphate sink that limits downstream signaling through PilG in lieu of a phosphatase (17, 18) or a separate response regulator controlling the function of the T4aP retraction ATPase PilT (12).

The Chp system positively regulates intracellular levels of cAMP by activating the major adenylate cyclase CyaB (17). Deletion of *pilG* results in decreased cAMP, surface piliation, and twitching motility, while *pilH* mutants have more cAMP and surface piliation but less twitching than the wild type (17). Supplementation of a *pilG* mutant with exogenous cAMP restored surface piliation but not twitching motility (17), suggesting that PilG regulates pilus biogenesis and function by at least two pathways. A recent study (18) showed that, of the two proteins, PilH is the preferred target of ChpA phosphorylation, consistent with its proposed role as a phosphate sink. Decreased twitching motility in the *pilH* background may reflect hyperphosphorylation of PilG, perturbation of the chemotactic response, and uncoordinated movement.

Important for *P. aeruginosa* virulence is its ability to switch from a planktonic to a sessile state when cells contact surfaces (19, 20). T4aP-mediated surface interaction is proposed to lead to signaling through the Chp system, upregulating surface-associated virulence phenotypes by increasing intracellular levels of cAMP (20). Vfr (virulence factor regulator) binds cAMP and modulates the expression of >200 genes, including genes for the type II secretion system (T2SS) and its effectors and T4aP assembly components, including the motor ATPases PilBTU, the alignment subcomplex PilMNOP, the secretin PilQ, and the PilSR two-component system that regulates PilA levels (21). This regulatory circuitry allows for just-in-time expression of components required for a surface-associated lifestyle in response to contact.

FimV is also required for T4aP function and CyaB activation (17) and is proposed to link into the Chp system via the cytoplasmic protein FimL (22). FimV is a 97-kDa inner membrane protein with one transmembrane segment. Its periplasmic domain contains a lysin (LysM) motif that binds peptidoglycan (PG) (23), and its cytoplasmic domain contains three discontinuous tetratricopeptide repeat (TPR) motifs involved in protein-protein interactions (24). FimV homologs have been identified in other T4P-producing bacteria (10), although their overall sequence identity is low, with the most conserved features being the LysM motif (COG3170), the single transmembrane segment, and a highly conserved cytoplasmic “FimV C-terminal domain”—TIGR03504—encompassing a single TPR and capping helix (25).

FimV homologs have been characterized in several species (8–11, 26–28), but their functions are not necessarily conserved. Deletion of FimV from *Legionella pneumophila* resulted in loss of twitching motility and cell elongation, while deletion of the *Neisseria meningitidis* FimV homolog TspA led to decreased host cell adhesion but had no effect on twitching motility or surface piliation. The *Vibrio cholerae* homolog, HubP, functions as a protein interaction hub, although its role is not limited to T4P localization. Deletion of HubP altered the cellular distribution of the chemotactic and flagellar machinery and the chromosomal origin, *oriCI* (28). HubP from *Shewanella putrefaciens* is responsible for localization of the chemotactic machinery but not the flagellar system (27). Yamaichi et

al. (28) showed that the polar localization of *V. cholerae* HubP is dependent on the conserved LysM motif (25). Wehbi et al. (29) showed that *P. aeruginosa* *fimV* mutants have decreased levels of the T4aP alignment subcomplex proteins PilMNOP, while in-frame deletion of FimV's LysM motif resulted in fewer PilQ multimers, suggesting that PG binding is important for optimal secretin formation. A recent study (30) confirmed that FimV participates in the localization of PilMNOPQ to sites of future cell division, ultimately placing T4aP assembly systems at both poles of newly divided cells.

T4aP-mediated twitching motility requires both cAMP-dependent and -independent inputs (17, 31). For example, provision of exogenous cAMP to mutants lacking PilG restored piliation but not motility (17), and a mutant expressing a constitutively active form of CyaB but lacking FimV failed to twitch (25). FimL was proposed to link PilG to the C-terminal TPR motif of FimV, leading to CyaB activation, and FimV localized both FimL and PilG to cell poles (22, 25). However, of these three proteins, only FimL is dispensable for twitching motility under cAMP-replete conditions. Thus, the FimV-FimL-PilG model fails to explain the cAMP-independent roles of FimV and PilG in twitching.

Here we provide evidence supporting different cAMP-independent roles for FimV and PilG in the regulation of twitching motility. We show that, in addition to the polar localization of FimL, PilG, and PilMNOPQ (22, 30), FimV is responsible for the polar localization of PilS, the membrane-bound sensor kinase that controls *pilA* transcription. These data show that FimV plays a central role in the control of twitching motility that overlaps—but is distinct from—that of the Chp system.

RESULTS

FimV is required for Chp activation of CyaB. FimL, FimV, and PilG are all required for activation of CyaB, with FimL proposed to link FimV to the Chp system through PilG (17, 22, 32, 33). However, while phenotypes associated with *fimL* deletion could be rescued by deletion of *cpdA* or by increasing intracellular cAMP levels in other ways (22, 33, 34), provision of exogenous cAMP failed to restore motility to a *pilG* mutant (17). We investigated whether the cAMP-independent function of PilG also required FimV by comparing PilU levels—a proxy for intracellular cAMP levels (21, 25)—twitching, and piliation in *fimL*, *fimV*, and *pilG* single mutants or in double mutants also lacking *cpdA* to prevent the degradation of endogenous cAMP (33) (Fig. 1). To confirm that FimV and FimL are epistatic to PilG, we also examined *pilH fimL* and *pilH fimV* double mutants. In the absence of PilH, cells are predicted to have hyperphosphorylated PilG, consistent with the high levels of cAMP observed in a *pilH* background (17, 18).

PilU levels were decreased in *fimL*, *fimV*, and *pilG* mutants, to 28, 10, and 22% of the wild-type level, respectively, consistent with previously described roles in the regulation of cAMP synthesis (Fig. 1) (10, 12, 17, 33). Both the *pilG* and *fimV* mutants were twitching deficient, while *fimL* mutant twitching resembled that of the wild type, as reported previously (33, 35). The *cpdA* mutant had high levels of PilU, surface piliation, and wild-type twitching, consistent with high cAMP levels (17, 33). Deletion of *cpdA* in the *fimL*, *fimV*, or *pilG* mutant increased PilU levels relative to those of the corresponding single mutants, to at least wild-type levels (Fig. 1), showing that CyaB retains residual activity in those mutant backgrounds. However, only the *cpdA fimL* mutant was motile, confirming that both PilG and FimV have cAMP-independent roles in T4aP function. Also consistent with previous reports (17), a *pilH* mutant assembled surface pili but was twitching impaired (~39% of the wild-type level). The *pilH fimV* and *pilH fimL* double mutants had PilU levels similar to those of *fimV* and *fimL* single mutants, suggesting that despite its hyperphosphorylation in the absence of *pilH* (18), PilG was unable to activate CyaB without FimV or FimL, confirming that all three are required for the Chp system to stimulate cAMP synthesis.

Decreased levels of PilMNOPQ in a *fimV* mutant are due to decreased cAMP. Wehbi et al. (29) showed previously that a *fimV* mutant had reduced levels of PilMNOP and that a *fimV_{LysM}* mutant with an in-frame deletion of the LysM motif had fewer PilQ secretins. However, transcription of the *pilMNOPQ* operon is Vfr dependent and thus cAMP dependent (21). To determine if any of these phenotypes are independent of

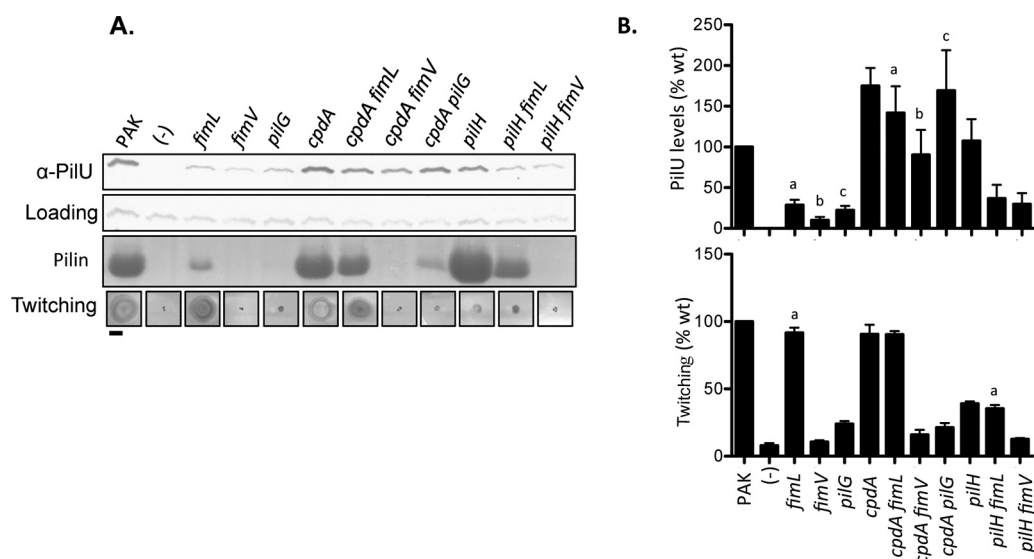


FIG 1 *FimV* and *PilG* have separate cAMP-independent roles in T4aP function. (A) Loss of *fimL* reduces the levels of PilU (a proxy for intracellular cAMP levels) (25), surface piliation, and twitching motility, and all phenotypes are restored to wild-type levels in a *cpdA fimL* double mutant. In contrast, the *fimV* and *pilG* mutants lack surface piliation and motility even in a *cpdA* background, even though PilU levels are restored to wild-type or greater levels. Negative controls (–) were *pilU* or *pilA* mutant bacteria, respectively. Scale bar = 1 cm. (B) Quantification of relative PilU levels and twitching zone diameters compared to those of wild-type (wt) PAK (set to 100%); measurements are the average of three experiments. Data were analyzed by repeated-measures ANOVA by using the single mutants as the control data set versus double mutants. Matching letters indicate statistically significant differences ($P < 0.05$).

cAMP, we examined levels of PilMNOPQ and PilU and twitching motility in a *fimV* mutant, a *fimV*_{LysM} mutant encoding only the cytoplasmic domain of *FimV* (*fimV*₁₁₉₄), and a *fimV* *cyaB*-R456L double mutant that expresses constitutively active *CyaB* (25, 36).

The fragments of *FimV* were stable (see Fig. S1 in the supplemental material), although—as reported previously (29)—expression levels could not be reliably quantified because of *FimV*'s aberrant migration on SDS-PAGE. The *fimV* mutant had low levels of PilU (~23% of the wild-type level), reflecting low cAMP levels, while the *fimV* *cyaB*-R456L double mutant had wild-type levels of PilU (Fig. 2). The *fimV*₁₁₉₄ mutant had ~29% of the wild-type PilU level, suggesting that even though its protein partners *PilG* and *FimL* are cytoplasmic, expression of *FimV*'s cytoplasmic domain alone was insufficient to activate *CyaB*. Complementation of the *fimV* and *fimV*₁₁₉₄ mutants in *trans* with a construct expressing full-length *FimV* increased PilU levels to ~58 and ~65% of the wild-type level, respectively. Surprisingly, the *fimV*_{LysM} mutant had ~89% of the wild-type PilU level, suggesting that the LysM motif, and thus PG binding, is dispensable for *CyaB* activation.

The *fimV* mutant had decreased levels of PilMNOP and few detectable PilQ multimers, and all were restored to wild-type levels with full-length *FimV*. Supporting the hypothesis that their expression levels are dependent on *Vfr* and cAMP, the *fimV* *cyaB*-R456L double mutant had wild-type levels of PilMNOPQ. However, the *fimV* *cyaB*-R456L double mutant had no recoverable surface pili (Fig. 2) and could not twitch, confirming a cAMP-independent role(s) for *FimV* in pilus assembly and twitching motility. The *fimV*₁₁₉₄ mutant had low levels of PilMNOP and low levels of PilQ multimers, but these could be rescued by complementation with full-length *FimV*. The *fimV*_{LysM} mutant had essentially wild-type PilMNOPQ levels and could assemble surface pili (Fig. 2); however, its twitching was ~37% of the wild-type level. The motility defect of the *fimV*_{LysM} mutant suggests that PG binding is important for *FimV*'s cAMP-independent function(s).

Wehbi et al. (29) showed that the *fimV*₁₁₉₄ mutant (which expresses the cytoplasmic domain of *FimV*) was unable to twitch, but motility could be rescued by complementation in *trans* with a construct expressing only the periplasmic domain of *FimV*

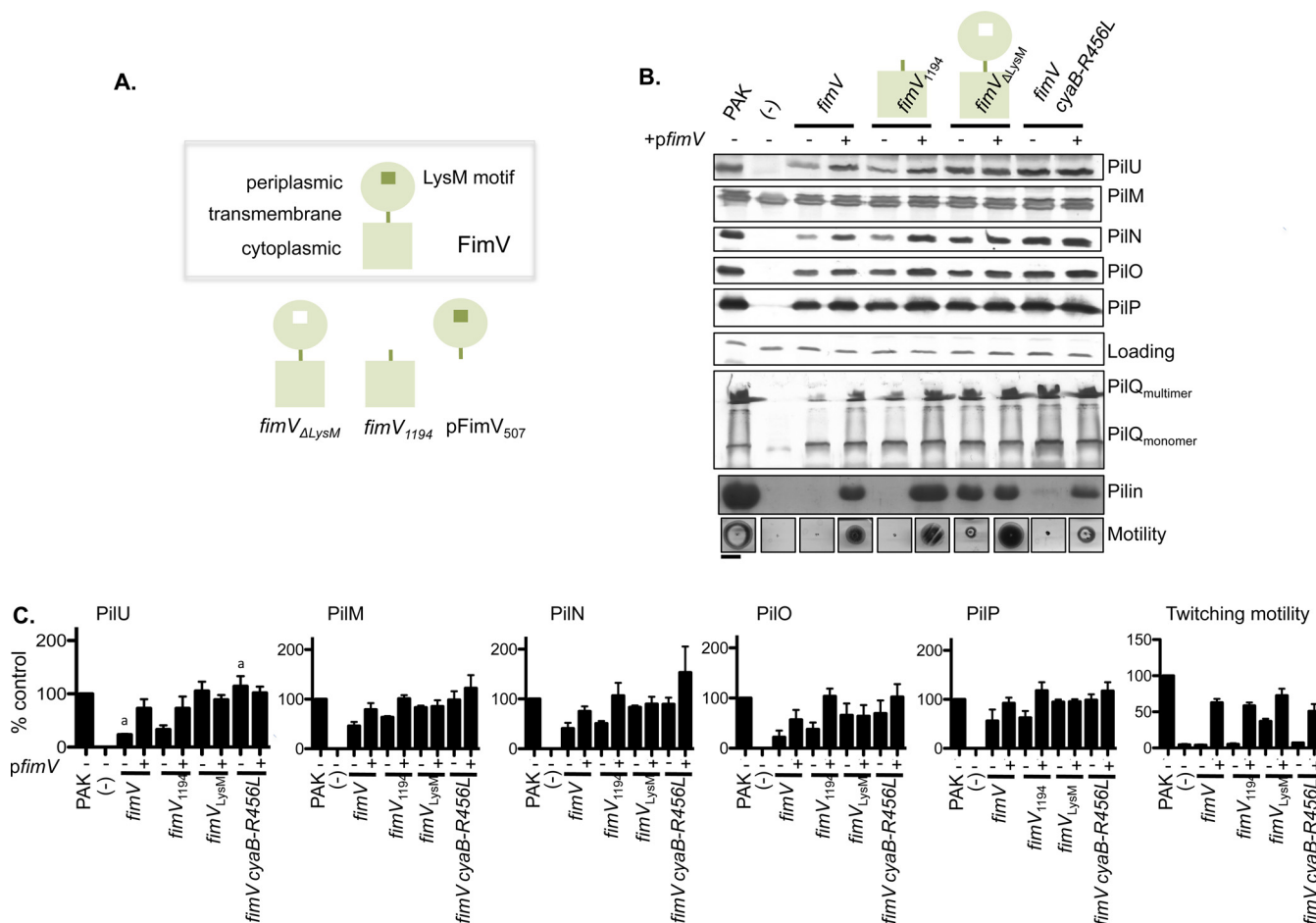


FIG 2 FimV and its LysM motif are essential for twitching motility. (A) Schematic of the FimV fragments used in this work. FimV's periplasmic and cytoplasmic domains are connected by a single transmembrane segment. The N-terminal periplasmic domain contains a PG-binding LysM motif (green square), which is deleted in frame in the *fimV*_{ΔLysM} mutant (white square). (B) The levels of PilU (a proxy for intracellular cAMP levels) (25) and assembly machinery components PilMNOPQ were assessed by Western blotting in various *fimV* mutant backgrounds complemented with the empty vector or with full-length *fimV*; a representative blot is shown. Surface piliation and twitching motility are shown in the bottom two rows. Scale bar = 1 cm. (C) Quantification of protein levels and motility in three independent experiments. Note that PilQ multimer levels cannot be accurately quantified by Western blot analysis. Statistically significant changes were identified with a paired *t* test. In the absence of *fimV*, levels of PilU, PilN, and PilO and PilQ multimers were reduced and surface piliation and motility were lost. These phenotypes were restored by complementation with *fimV* in *trans*. The *fimV*₁₁₉₄ mutant expressing only the cytoplasmic domain phenocopied the *fimV* deletion mutant. When FimV's LysM motif was deleted, the levels of the proteins of interest and piliation were similar to those of the wild type but motility remained severely impaired. CyaB requires FimV for its activity, but in the absence of *fimV*, it can be constitutively activated by an R456L mutation (36). However, the cells have very few surface pili and are nonmotile. Mutants lacking *pilU*, *pilM*, *pilN*, *pilO*, *pilP*, *pilQ*, and *pilA* were used as negative controls (–) for relevant immunoblot assays.

(residues 1 to 507, pFimV₅₀₇), suggesting that, together, the two FimV fragments could restore function without being physically connected. A *fimV* deletion mutant complemented with the empty vector or pFimV₅₀₇ had similarly low PilU levels, suggesting that the periplasmic domain alone is not sufficient to activate CyaB (Fig. 3A). Unexpectedly, despite its ability to restore motility in the *fimV*₁₁₉₄ background (Fig. 3B), pFimV₅₀₇ did not significantly increase PilU levels in that background, suggesting that the cytoplasmic and periplasmic domains cannot activate CyaB efficiently when they are not covalently linked. However, CyaB activation is not strictly required for twitching, as both the *fimL* (Fig. 1) and *cyaAB* mutants have low cAMP levels and piliation but nearly wild-type motility (17, 33). We next tested if FimV's periplasmic domain plays a cAMP-independent role in twitching by complementing the *fimV* *cyaB*-R456L mutant with pFimV₅₀₇. pFimV₅₀₇ failed to restore twitching in the *fimV* *cyaB*-R456L double mutant (Fig. 3B), suggesting that the cytoplasmic region of FimV plays a cAMP-independent role in motility. Taken together, the data show that the cAMP-independent role(s) of FimV requires both its periplasmic and cytoplasmic domains.

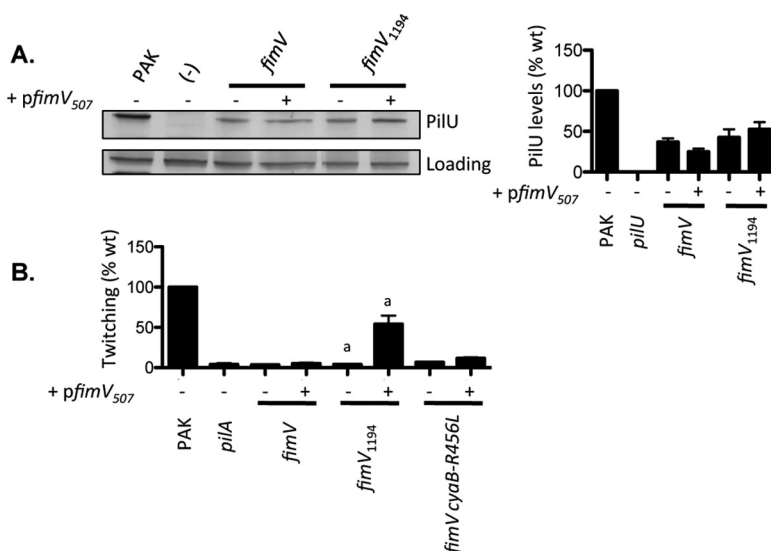


FIG 3 CyaB activation—but not twitching motility—requires that FimV's cytoplasmic and periplasmic domains be connected. (A) Representative Western blot analysis of whole-cell lysates with anti-PilU antiserum and quantification of PilU levels (a proxy for cAMP levels) by densitometry ($n = 3$). The reduced levels of PilU in the *fimV* and *fimV*₁₁₉₄ mutants are not restored to wild-type (wt) levels by in-trans expression of the N-terminal domain (FimV₅₀₇). A mutant lacking *pilU* was used as the negative control. (B) Quantification of twitching motility. As reported previously (29), expression of pFimV₅₀₇ in trans complements motility in the *fimV*₁₁₉₄ mutant, which expresses only the cytoplasmic domain of FimV. It cannot complement the motility of a *fimV* deletion mutant, even when cAMP levels are restored by expressing constitutively active CyaB-R456L. Data were analyzed by paired *t* test with GraphPad Prism.

FimV is required for PilS localization. The *V. cholerae* homolog of FimV, HubP, interacts with multiple proteins and has a broad regulatory function (28). FimV is required for bipolar localization of PilG and FimL and the T4aP structural proteins PilMNOPQ but not the Chp methyl-accepting chemotaxis protein (MCP) PilJ (22, 30). To determine if FimV is required for the localization of other T4aP regulators, we examined its effects on the localization of PilS (37, 38), the histidine sensor kinase component of the PilRS two-component system that regulates *pilA* transcription in response to changes in PilA levels in the inner membrane (39).

In wild-type cells, PilS-yellow fluorescent protein (YFP) was localized to both poles (Fig. 4A), as reported previously (37), while in the absence of FimV, PilS-YFP was diffuse in the cell envelope. Interestingly, the localization pattern of PilS-YFP in the *fimV*_{LysM} mutant was similar to that in the wild type, suggesting that PG binding is not critical for PilS localization. However, PilS-YFP was mislocalized in the *fimV*₁₁₉₄ mutant, suggesting that the cytoplasmic domain is insufficient for PilS localization. Finally, because PilG also has cAMP-independent effects on motility (17) (Fig. 1), we examined PilS-YFP localization in a *pilG* mutant. Localization was similar to that of the wild type, further supporting the idea that PilG and FimV have distinct cAMP-independent roles in motility (Fig. 4A). These data also suggest that PilS localization is independent of the intracellular cAMP concentration. Despite differences in the brightness of PilS-YFP across strains, its expression levels were equivalent (Fig. 4B).

FimV deletion affects neither swimming nor swarming motility. As the *V. cholerae* and *S. putrefaciens* homologs of FimV modulate swimming motility (27, 28), we tested whether loss of *P. aeruginosa* *fimV* impairs swimming in a plate-based assay. We saw no effect of FimV deletion on swimming motility (Fig. 5), suggesting that it is not essential. Consistent with reports that swimming is negatively regulated by high cAMP levels (21), the *cpdA* mutant was swimming impaired (~53% relative to the wild type). Deletion of *cpdA* in the *fimV* (~77%), *fimL* (~90%), and *pilG* (~85%) backgrounds reduced swimming relative to that of the single mutants, probably because of increased cAMP levels (Fig. 1). Surprisingly, despite having very high cAMP (17) and piliation levels—similar to

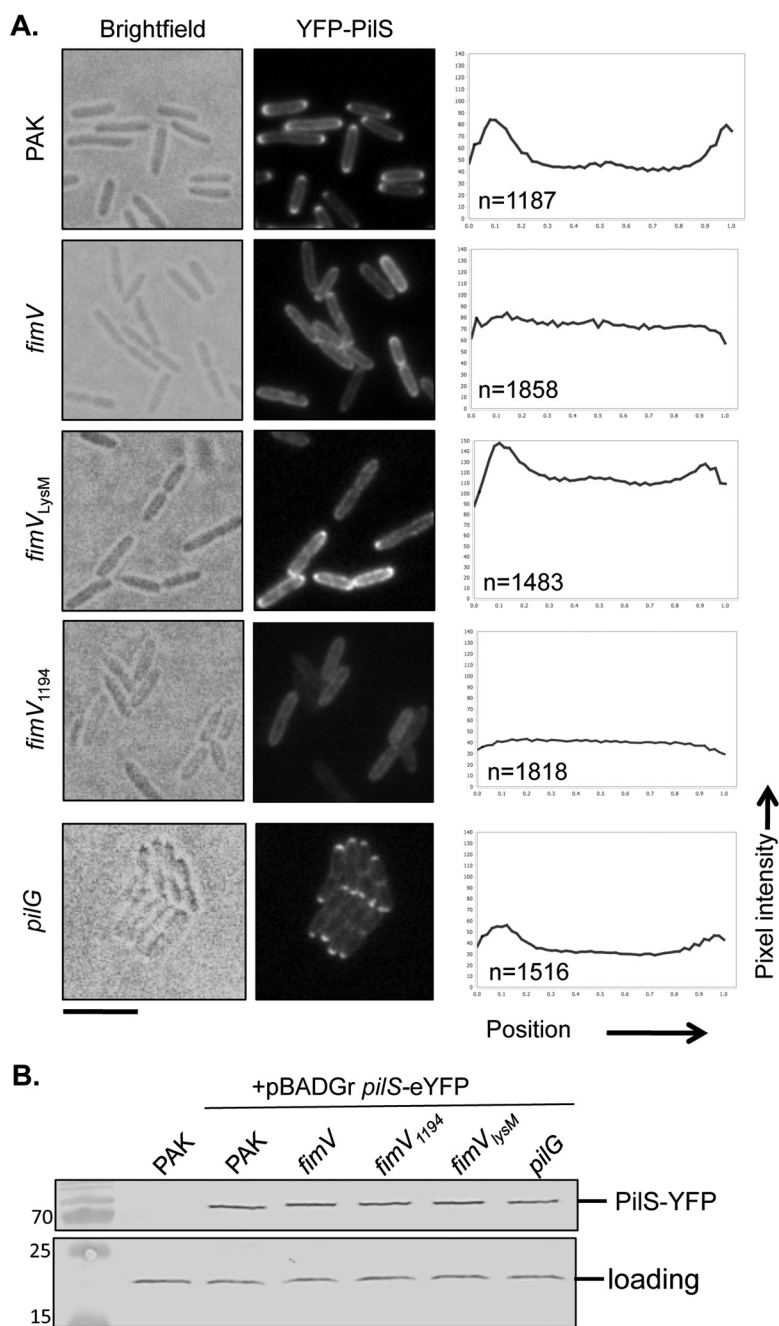


FIG 4 PilS localization depends on FimV. (A) Bright-field microscopy and fluorescence microscopy were used to image PilS-YFP localization in the wild type, *fimV* mutants, or a *pilG* mutant, and the average pixel intensity of the YFP signal along the long axis of the cell was quantified with MicrobeJ (51). The number of cells averaged for each population is shown on each graph. PilS-YFP is localized to the poles in wild-type cells, but fluorescence becomes circumferential in the *fimV* and *fimV₁₁₉₄* mutant backgrounds. In a mutant expressing FimV with an in-frame deletion of its LysM PG-binding motif, fluorescence is polar but patchy circumferential fluorescence is also visible. PilS-YFP remains polar in a *pilG* mutant. Scale bar = 5 μ m. (B) Representative Western blot analysis of whole-cell lysates with an anti-YFP antibody. Levels of PilS-YFP were equivalent in all strains. A cross-reactive protein was used as the loading control. The values to the left are molecular sizes in kilodaltons.

those of the *cpdA* mutant—when grown on 1.5% agar (Fig. 1), the *pilH* mutant had ~93% of the swimming motility of the wild type in 0.25% agar plates (Fig. 5A). To determine whether the growth of the *pilH* mutant under low-viscosity conditions and thus a potential lack of a contact-dependent increase in cAMP explained its failure to

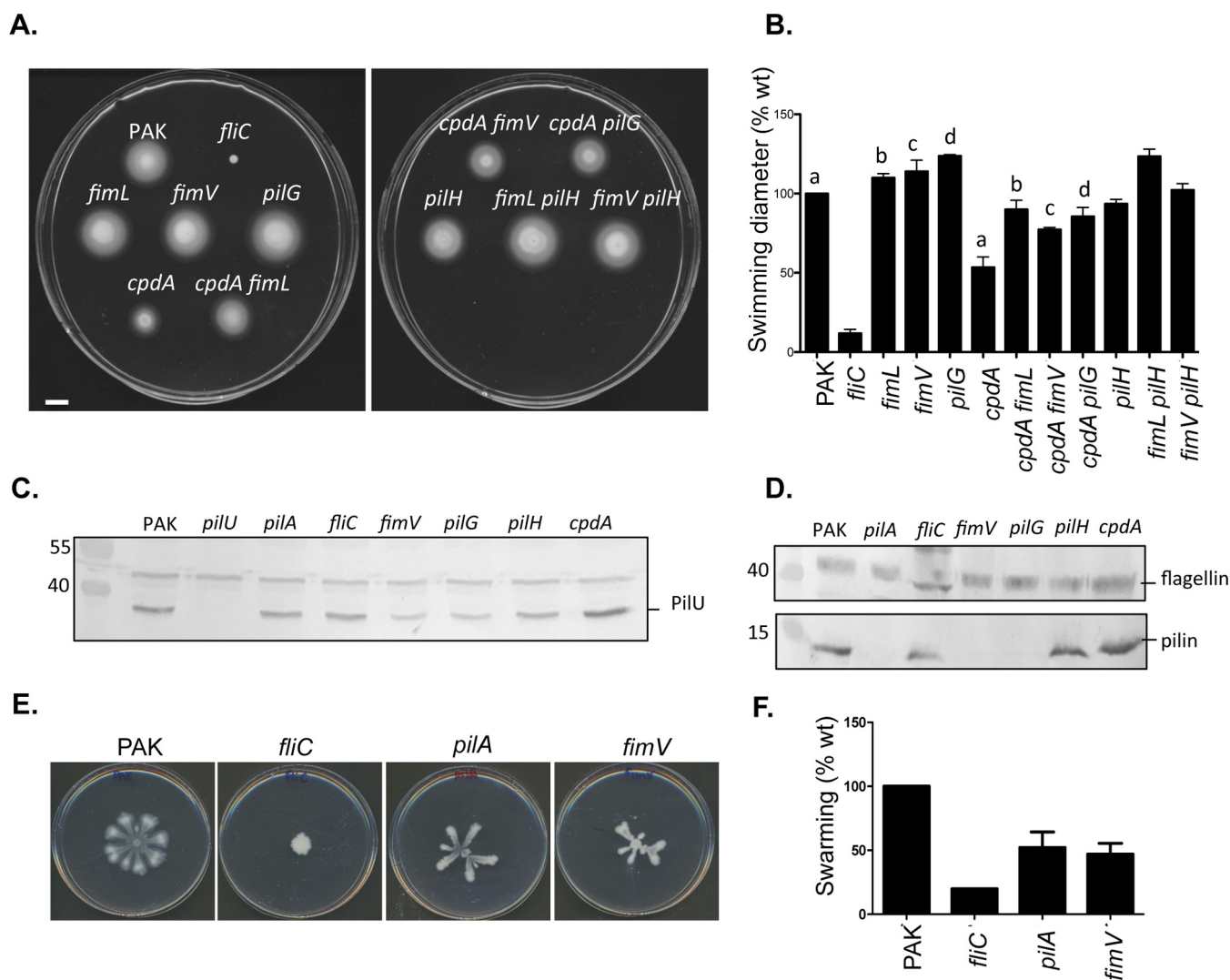


FIG 5 Swimming and swarming motilities of wild-type (wt) and mutant PAK strains. (A) Representative assays of swimming motility in 0.3% LB agar. Scale bar = 1 cm. (B) Quantification of swimming zones (average of three experiments). Lowercase letters indicate paired samples that are statistically significantly different from one another as measured by ANOVA by using the single mutants as the control data set when comparing the double mutants in the appropriate background. Loss of *fimV* does not impact swimming motility. PAK is the parent strain; the *fliC* mutant that lacks flagellin was included for comparison. (C, D) Representative Western blot assays of whole-cell lysates from strains grown in liquid medium with anti-PilU antiserum (C) and of sheared surface protein preparations with an antibody raised against sheared proteins (recognizes both pilins and flagellins) (D). The values to the left are molecular sizes in kilodaltons. Piliation levels are similar to those of samples prepared from solid medium (Fig. 1). (E) Representative swarming zones. (F) Quantification of swarming zones (average of three experiments).

phenocopy the *cpdA* mutant, the levels of PilU and sheared surface proteins were determined in cells isolated from broth cultures (Fig. 5C and D). The levels of PilU in broth-grown *pilG*, *pilH*, *fimV*, and *cpdA* mutants were all similar to those in plate-grown cells, and the levels of surface pili in the broth-grown *pilH* and *cpdA* mutants were similar to one another. Together, the data suggest that high levels of cAMP and piliation do not necessarily inhibit swimming motility.

The polar flagellum and T4P also play a role in swarming motility (40). Loss of *fliC* reduced swarming to ~20% of the wild-type level, while loss of *pilA* reduced swarming by about half (~52%) (Fig. 5E and F). Swarming of the *fimV* mutant was also impaired by ~47%, a reduction consistent with its lack of piliation. We conclude that *fimV* is not required for flagellar function in either swimming or swarming motility.

DISCUSSION

PilG, FimL, and FimV were proposed to be components of a surface-sensing pathway that activates CyaB (22), with FimL acting as a scaffold protein connecting PilG to FimV.

Consistent with this model, increasing the level of PilG phosphorylation through deletion of *pilH* (18) failed to increase levels of PilU if either FimV or FimL was missing (Fig. 1). However, only the *fimL* mutant twitched (Fig. 1) following the introduction of compensatory mutations that increased cAMP levels (17, 33), confirming that both PilG and FimV have cAMP-independent roles in twitching (17, 25). Thus, FimL's role in twitching is limited to its ability to connect PilG and FimV, leading to CyaB activation via an as-yet-unknown mechanism. Interestingly, Nolan et al. (34) identified other suppressors of *fimL* that mapped outside the *cyaA*, *cyaB*, *pilG*, *pilH*, *vfr*, and *cpdA* loci. How those uncharacterized loci fit into the FimV-FimL-PilG signaling axis remains to be determined.

Since FimL's role is limited to the cAMP-dependent pathway (22, 33) and twitching motility in the *fimL* background is essentially the same as that of the wild type (Fig. 1), PilG and FimV both function—together or independently of one another—in its absence. PilG polar localization is dependent on FimV, but PilG remains localized to the poles when FimL is absent (22). These data imply that PilG interacts with FimV directly or indirectly via another, as-yet-unidentified, adaptor protein. That component is unlikely to be part of the Chp system; the MCP PilJ localizes to the poles independently of FimV, and PilG retains bipolar localization in the absence of both PilJ (see Fig. S2) and the Chp system kinase ChpA (22). Identifying this interaction partner—potentially among the list of proteins recovered in a recent PilG pulldown-mass spectrometry study (22)—could help to clarify how PilG contributes to cAMP-independent regulation of twitching.

Because restoration of cAMP levels in a *pilG* mutant by supplying exogenous cAMP (17), constitutively activating CyaB (36), or deletion of *cpdA* (Fig. 1A) restores piliation but not twitching motility, the cAMP-independent role of PilG may be the coordination of pilus extension/retraction dynamics to permit directional movement. In *M. xanthus*, the Chp-like Frz system controls the asymmetric subcellular distribution of the PilB and PilT motor ATPases in cells undergoing T4aP-mediated S motility to coordinate movement (41). It is likely that asymmetric T4aP extension/retraction dynamics similarly occur in *P. aeruginosa*, as pilus retraction at both poles simultaneously would result in zero net movement.

How PilG might regulate pilus retraction remains unclear. CheY interacts with FliM at the *E. coli* flagellar switch complex to control the direction of flagellum rotation (42), but the T4aP system lacks an obvious FliM equivalent. However, the T4aP system was recently shown to have a rotary motor whose direction of rotation dictates pilus extension versus retraction (43–45). A single hexameric PilB or PilT ATPase docks in the PilM ring at the base of the apparatus and encircles the cytoplasmic domains of the PilC platform protein (7), rotating it clockwise or counterclockwise, respectively, to insert or extract pilin subunits from the pilus in a stepwise manner (45). Transient interactions of phospho-PilG with PilM, PilC, or the motor ATPases might dictate which ATPase is docked at the leading versus the lagging pole.

Interestingly, the cAMP-independent role of PilG appears to be dependent upon, but distinct from, that of FimV. In addition to FimL and PilG (22), FimV is required for polar localization of the structural components PilMNOPQ (30) and the PilSR two-component system (Fig. 4). However, unlike in *V. cholerae* and *S. putrefaciens* (27, 28), its deletion does not affect swimming in semisolid medium or swarming, another flagellum-dependent form of motility (Fig. 5). Swimming motility in *P. aeruginosa* is controlled in part by FlhF, which is required for polar recruitment of the Che machinery (46). Interactions between *V. cholerae* HubP and FlhF have been reported (28); whether similar interactions occur in *P. aeruginosa* remains to be determined. FimV and its homologs are emerging as protein interaction hubs that use LysM motifs to target themselves and their partners to the division septum, ensuring the correct placement of polar and partitioning systems during and after the separation of daughter cells (28, 30). Although studies of *L. pneumophila* FimV and *N. meningitidis* TspA (9, 11) did not address the role of the LysM motif or localization in function, the phenotypes of

mutants lacking these proteins could reflect mislocalization of motility or adhesion systems.

Septal PG binding by FimV was dispensable for CyaB activation (Fig. 2) even though FimL, PilG, and CyaB are all polar components (22, 33). Deletion of the LysM motif alone may not completely delocalize FimV, as it probably has other interaction partners that help to confine it to the cell poles; attempts to test this hypothesis with a FimV_{LysM}-YFP fusion have not been successful to date. Alternatively, sufficient FimV_{LysM} may be present at the cell pole to promote CyaB activity because of random diffusion in the inner membrane. Consistent with only partial mislocalization of FimV_{LysM}, PilS-YFP remained localized mostly to the poles in that background, while deletion of FimV's entire periplasmic region led to PilS delocalization (Fig. 4). Transmembrane domains 5 and 6 of PilS (47) and the membrane-embedded MASE2 domain of CyaB (36) are sufficient for their polar localization. Whether the short periplasmic loops of PilS (47) interact with the periplasmic domain of FimV is unknown. PilS, CyaB, and FimV could interact via their transmembrane segments or be integrated in a signaling hub through as-yet-unidentified intermediaries.

In summary, this work helps to resolve the cAMP-dependent and -independent regulation of *P. aeruginosa* twitching motility by FimV and PilG. The cAMP-independent role of FimV is likely to coordinate the localization of multiple T4aP structural and regulatory components to the cell poles, while that of PilG may be to coordinate pilus retraction in a way that allows directional movement; experiments to test this idea are under way. Characterization of the FimV protein interaction network will identify its full repertoire of direct and indirect interaction partners and clarify the links between polar localization and function.

MATERIALS AND METHODS

Bacterial growth and culture conditions. The bacterial strains and plasmids used in this study are listed in Table 1. Unless otherwise stated, *P. aeruginosa* strains and all *E. coli* strains were grown on LB agar at 37°C. Antibiotic selection was as follows unless stated otherwise: gentamicin (Gm), 15 µg/ml for *E. coli* and 30 µg/ml for *P. aeruginosa*; kanamycin, 50 µg/ml for *E. coli*; ampicillin, 100 µg/ml for *E. coli*. All *P. aeruginosa* strains containing a FimV complementation construct were grown on medium supplemented with 0.1% (wt/vol) arabinose.

Mutant generation. Mutants were made as previously described (17). Deletion constructs for the generation of *fimL*, *cpdA*, and *fimV* mutants were designed to include 1,000 nucleotides upstream and downstream of the gene to be deleted. The *pilH* deletion construct was designed to include the first 12 and last 30 nucleotides of the gene. The upstream and downstream fragments were amplified from the PAK chromosome with the primer sets described in Table 2. Inserts were cloned into the pEX18Gm suicide vector at the SacI and HindIII sites (pEX18Gm::*fimL*), KpnI and EcoRI sites (pEX18Gm::*cpdA*), and HindIII and KpnI sites (pEX18Gm::*pilH*). Suicide vectors were verified by DNA sequencing.

After verification, plasmids (pEX18Gm::*fimL*, pEX18Gm::*cpdA*, pEX18Gm::*pilH*, and pEX18Gm::*fimV*_{LysM}) were transformed into *E. coli* SM10 cells. Plasmids were transferred to *P. aeruginosa* by conjugation at a 6:1 ratio of *E. coli* to *P. aeruginosa*. A 100-µl volume of the 6:1 mixed culture was spotted onto LB 1.5% (wt/vol) agar and incubated overnight at 37°C. The mating mixture was resuspended in 5 ml of LB, and 100 µl was plated onto *Pseudomonas* isolation agar supplemented with Gm at 100 µg/ml and grown overnight at 37°C. Single colonies were resuspended in 1 ml of LB, plated onto LB 1.5% agar lacking sodium chloride and supplemented with 8% (wt/vol) sucrose, and grown overnight at 30°C. Resulting single colonies were replica plated onto LB and LB supplemented with Gm at 30 µg/ml. Mutants were verified by PCR, and the *pilH* mutant was screened by Western blotting with anti-PilH antiserum. Double mutants were generated in the same manner.

Plasmid construction. The coding region of the first 507 residues of FimV was amplified by PCR with pBADGr::*fimV* as a template and cloned into pBADGr. The PCR-amplified DNA was digested with KpnI and XbaI, purified, and ligated into pBADGr at the KpnI and XbaI sites with T4 DNA ligase in accordance with the manufacturer's instructions (Thermo Scientific). A version of *pilS* lacking its stop codon was amplified from the PAK chromosome and cloned into pBADGr::*yfp* in frame with *yfp* at the EcoRI and SmaI sites. In-frame ligation was confirmed by DNA sequencing. A version of *pilG* lacking its stop codon was amplified from the PAO1 chromosome and cloned into the pMarkIC vector, which encodes (Gly₃-Ser)₃-YFP at the HindIII site of pUCP20Gm. *pilG* was ligated into the EcoRI and XbaI sites. In-frame ligation was confirmed by DNA sequencing.

Immunoblotting. Western blotting of whole-cell lysates was performed as previously described (48). In brief, whole-cell lysates were prepared from strains grown overnight on LB 1.5% agar or, in the case of plasmid-transformed strains, LB 1.5% agar supplemented with 0.1% (wt/vol) arabinose. Cells were then resuspended in 1× phosphate-buffered saline (PBS) and normalized to an optical density at 600 nm (OD₆₀₀) of 0.6. Cells were pelleted by centrifugation at 2,300 × *g* for 5 min. Pellets were then resuspended in 175 µl of 1× SDS-PAGE loading dye. Cell lysates were resolved by 15% SDS-PAGE and transferred to

TABLE 1 Strains and plasmids used in this study

Strain or plasmid	Genotype/description	Source or reference
<i>P. aeruginosa</i>		
PAK	Wild-type <i>P. aeruginosa</i> K strain	17
NP	PAK with deletion of <i>pilA</i>	53
<i>pilU</i> mutant	PAK with deletion of <i>pilU</i>	25
<i>fimV</i> mutant	PAK with deletion of <i>fimV</i>	25
<i>fimV</i> _{LysM} mutant	PAK with in-frame deletion of LysM motif, nucleotides 519–690	This study
<i>fimV</i> <i>cydB</i> -R456L mutant	PAK with deletion of <i>fimV</i> and arginine-to-lysine substitution in <i>cydB</i> at position 456	25
<i>fimV</i> ₁₁₉₄ mutant	PAK with FRT insertion at nucleotide position 1194 in <i>fimV</i>	29
<i>fimL</i> mutant	PAK with deletion of <i>fimL</i>	This study
<i>pilG</i> mutant	PAK with deletion of <i>pilG</i>	17
<i>cpdA</i> mutant	PAK with deletion of <i>cpdA</i>	This study
<i>cpdA</i> <i>fimV</i> mutant	PAK with deletions of <i>cpdA</i> and <i>fimV</i>	This study
<i>cpdA</i> <i>fimL</i> mutant	PAK with deletions of <i>cpdA</i> and <i>fimL</i>	This study
<i>cpdA</i> <i>pilG</i> mutant	PAK with deletions of <i>cpdA</i> and <i>pilG</i>	This study
<i>pilH</i> mutant	PAK with deletion of <i>pilH</i>	This study
<i>pilH</i> <i>fimV</i> mutant	PAK with deletions of <i>pilH</i> and <i>fimV</i>	This study
<i>pilH</i> <i>fimL</i> mutant	PAK with deletions of <i>pilH</i> and <i>fimL</i>	This study
<i>E. coli</i>		
DH5 α	F [−] ϕ 80 <i>dlacZ</i> Δ M15 Δ (<i>lacZYA-argF</i>)U169 <i>recA1</i> <i>endA1</i> <i>hsdR17</i> (r _K [−] m _K ⁺) <i>phoA</i> <i>supE44</i> <i>thi-1</i> <i>gyrA96</i> <i>relA1</i> λ [−] ; general cloning strain	Invitrogen
SM10	<i>thi-1</i> <i>thr</i> <i>leu</i> <i>tonA</i> <i>lacY</i> <i>supE</i> <i>recA</i> ::RP4-2 Tc ^r ::Mu Km ^r ; mating donor strain	54
Plasmids		
pBADGr	Arabinose-inducible expression vector	55
pBADGr:: <i>fimV</i>	Arabinose-inducible expression construct encoding full-length FimV	25
pBADGr:: <i>fimV</i> ₅₀₇	Arabinose-inducible expression construct encoding periplasmic domain of FimV, residues 1–507	This study
pEX18Gm:: <i>fimL</i>	Suicide vector containing 1 kb upstream and downstream of <i>fimL</i> locus	This study
pEX18Gm:: <i>cpdA</i>	Suicide vector containing 1 kb upstream and downstream of <i>cpdA</i> locus	This study
pEX18Gm:: <i>pilH</i>	Suicide vector containing 1 kb upstream and downstream of <i>pilH</i> locus	This study
pEX18Ap- <i>fimV</i> -GmFRT	Suicide vector containing <i>fimV</i> amplified from PAO1 and disrupted at nucleotide position 1194 with FRT-flanked gentamicin resistance cassette	29
pEX18Gm- <i>fimV</i> _{LysM}	Suicide vector containing residues 1–1521 of <i>fimV</i> with deletion of nucleotides 519–690	29
pBADGr::eYFP(HindIII)	Arabinose-inducible expression construct encoding eYFP cloned into HindIII site	30
pBADGr::PilS-YFP	Arabinose-inducible expression construct with <i>pilS</i> cloned upstream of eYFP	This study
pMarkiC	puCP20Gm-based vector with (Gly ₃ -Ser) ₃ -YFP cloned into HindIII site	This study
pMarkiC:: <i>pilG</i>	pMarkiC with <i>pilG</i> cloned into EcoRI and XbaI sites	This study

nitrocellulose membranes. Membranes were blocked in 5% skim milk dissolved in PBS (pH 7.4) for 1 h, washed in PBS, and incubated with PBS-diluted antiserum raised against the FimV periplasmic domain (1:1,000), PilU (1:5,000), PilM (1:1,000), PilN (1:1,000), PilO (1:1,000), PilP (1:1,000), or PilQ (1:1,000) or an anti-GFP polyclonal antibody (Novus Biologicals; 1:5,000) for 1 h, washed, incubated with an alkaline

TABLE 2 Oligonucleotides used in this study

Primer	Sequence
FimV-F	5'-GCGGGTACCATGGTTCGGCTTCGTACACTGGTTCGGG-3'
FimV ₅₀₇ -R	5'-GCGTCTAGACTAGTGGTGATGGTGATGCTGTCCTCGCCGGTATCCGCGGC-3'
PilS YFP-F	5'-GACGAATTCATGCGCGCTGAACGGCTA-3'
PilS YFP-R	5'-GCACCCGGGTGCTGAGTTTTCGTGGGTGGGC-3'
ko FimL F1	5'-CGCGAGCTCAATGGGCGTGCCGTGCATCA-3'
ko FimL R1	5'-CGCGGATCCCGGTCTAGTGCCTCC-3'
ko FimL F2	5'-CGCGGATCCTGCGCGGCGAGTTCCGT-3'
ko FimL R2	5'-CGCAAGCTTGACCGTCAGCTCGCTGCTC-3'
ko cpdA F1	5'-TCAAGCTTGGATCAGCTCGACGCCCGCA-3'
ko cpdA R1	5'-TCGGTACCTCTCGAAGTGGACTACGACA-3'
ko cpdA F2	5'-TACGGTACCAGGCGTGGTGGCGGGAGT-3'
ko cpdA R2	5'-TCGAATTCACGACCGCAGCGGATTGC-3'
ko pilH F1	5'-GCGAAGCTTCGTTATCGAAGGGCGGGTCC-3'
ko pilH R1	5'-GGGTCTAGAATCAACAATCAAAATACGAGCCATGGGG-3'
ko pilH F2	5'-GGGTCTAGAAATGCGGTGCTGGCGGGTGA-3'
ko pilH R2	5'-GCGGGTACCCGTTTCTCGAAGTCGTTGCG-3'
G_MarkiC_F	5'-ATTTAAGAATTGAGGAGGATATATGGAACAGCAATCCGACG-3'
G_MarkiC_R	5'-AATCATTTAGAGGAAACGGCGTCCACCGGG-3'

phosphatase-conjugated goat anti-rabbit secondary antibody (1:3,000; Bio-Rad) for 1 h, and washed. Blots were developed with 5-bromo-4-chloro-3-indolylphosphate and nitroblue tetrazolium. Data are representative of three independent experiments.

Sheared surface protein preparation. Surface pili were analyzed as previously described (49). In brief, strains of interest were streaked in a grid-like pattern onto LB 1.5% agar or, in the case of plasmid-transformed strains, LB 1.5% agar supplemented with 0.1% (wt/vol) arabinose and grown overnight at 37°C. Cells were gently scraped from the plates with a sterile coverslip and resuspended in 4.5 ml of PBS (pH 7.4). Surface appendages were sheared by vortexing the cells for 30 s. The OD₆₀₀ of each strain was measured, and an amount of cells equivalent to 4.5 ml of the sample with the lowest OD₆₀₀ was pelleted by centrifugation at 16,100 × *g* for 5 min. When necessary, PBS was added to samples to a final volume of 4.5 ml prior to centrifugation. Supernatants were removed and centrifuged again at 16,100 × *g* for 20 min to remove the remaining cells. Supernatants were collected, mixed with 5 M NaCl and 30% (wt/vol) polyethylene glycol (Sigma; molecular weight, ~8,000) to a final concentration of 0.5 M NaCl and 3% (wt/vol) polyethylene glycol, and incubated on ice for 30 min. Precipitated surface proteins were collected by centrifugation at 16,100 × *g* for 30 min. Supernatants were discarded, and samples were centrifuged again at 16,100 × *g* for 2 min. Pellets were resuspended in 150 μl of 1× SDS-PAGE sample buffer (80 mM Tris [pH 6.8], 5.3% [vol/vol] 2-mercaptoethanol, 10% [vol/vol] glycerol, 0.02% [vol/vol] bromophenol blue, 2% [vol/vol] SDS). Samples were boiled for 10 min and resolved by 15% SDS-PAGE. Bands were visualized by staining with Coomassie brilliant blue (Sigma). Data are representative of three independent experiments.

Twitching assay. Twitching motility was tested as previously described (49). In brief, cells from an overnight culture were stab inoculated into the interface between LB 1% agar or, in the case of plasmid-transformed strains, LB 1% agar supplemented with 0.1% (wt/vol) arabinose and the underlying tissue culture-treated polystyrene petri dish and incubated at 37°C for 16 h (Thermo Fisher). Twitching zones were visualized by removing the agar, staining the cells on the petri dish with 1% (wt/vol) crystal violet, and washing them with water to remove unbound dye. Twitching zones were measured by analyzing the diameter of each twitching zone in pixels with ImageJ software (NIH). Twitching zones were normalized to the twitching diameter of wild-type PAK in each individual experiment. Data are representative of three independent experiments, with one colony used in each experiment.

Fluorescence microscopy. *P. aeruginosa* strains transformed with pBADGr::FimV-eYFP were grown overnight. Microscopy was performed with an eight-well 1.0 borosilicate chambered coverglass (LabTek). Chamber slides were prepared by adding LB 1% agar supplemented with 0.1% (wt/vol) arabinose to create an agar layer ~3 mm thick covering the bottom of the chamber. Agar was allowed to solidify with the lid off to prevent condensation. Bacteria were stab inoculated into the interface between the agar and the coverglass. Slides were wrapped in foil to prevent photobleaching and incubated at 37°C for 1 h in the dark. Cells were then imaged with an EVOS FL Auto microscope with a monochrome camera for bright-field imaging and a YFP LED light cube for fluorescence imaging through a 60× oil immersion objective at room temperature. Representative fields were cropped from larger images and enlarged with ImageJ software (NIH) (50).

Fluorescence images were quantified with the MicrobeJ plug-in for ImageJ (51). Bright-field and fluorescence images were arranged into a stack in ImageJ. Regions of interest corresponding to the bacteria were selected on the basis of the bright-field image and thresholding of particles on the basis of length (0.5 to 5 μm), width (0.2 to 1.5 μm), area (0.75-μm² maximum), and fit to rod-shaped bacteria. Pixel intensity profiles were generated by MicrobeJ by using the profile option on the fluorescence image with a 1-μm width and 0.5-μm extensions. Intensity profiles were plotted along the *y* axis with a range of 0 to 140, and the axis was partitioned into 50 bins. Pixel intensity profiles were generated for the YFP channel. Data are representative of at least three independent trials.

Swimming and swarming assays. For swimming assays, cells from overnight cultures were resuspended in sterile PBS and standardized to an OD₆₀₀ of 0.6. Two microliters of a cell suspension was spotted onto LB 0.3% agar and allowed to dry onto the surface of the agar. Plates were incubated at 30°C for 16 h with the agar side down. Data are representative of three independent experiments with single colonies inoculated onto each plate.

Swarming motility assays were conducted as described by Köhler et al. (52), with some modifications. Briefly, strains of interest were grown overnight at 37°C in 5 ml of LB. The following day, swarming plates were prepared with 10× M8 salts (12.8% [wt/vol] Na₂HPO₄·7H₂O, 3% KH₂PO₄, 0.5% NaCl [pH 7.4]) diluted to a final concentration of 1× and 0.5% agar. After autoclaving and cooling to ~60°C, the medium was supplemented with 2 mM MgSO₄, 0.2% glucose, 0.05% L-glutamic acid, and trace elements (composition available upon request). Petri dishes were filled with 20 ml of medium per plate and allowed to solidify at room temperature for 1.5 h. From each of the overnight cultures, 3.5 μl of inoculum was then spotted at the center of each plate and the plates were incubated upright at 30°C in a controlled-humidity incubator for 48 h. Quantification was performed by measuring swarming zone areas with ImageJ (50).

Statistical analyses. Data were analyzed by analysis of variance (ANOVA) or Student's *t* test where appropriate, as indicated in the figure legends, with GraphPad Prism.

SUPPLEMENTAL MATERIAL

Supplemental material for this article may be found at <https://doi.org/10.1128/JB.00188-17>.

SUPPLEMENTAL FILE 1, PDF file, 5.3 MB.

ACKNOWLEDGMENTS

This study was supported by grant MOP-93585 from the Canadian Institutes of Health Research (CIHR) to P.L.H. and L.L.B. P.L.H. holds a Tier I Canada Research Chair. S.L.N.K. was the recipient of an Ontario Graduate Scholarship.

REFERENCES

- Albers SV, Pohlschroder M. 2009. Diversity of archaeal type IV pilin-like structures. *Extremophiles* 13:403–410. <https://doi.org/10.1007/s00792-009-0241-7>.
- Pellic V. 2008. Type IV pili: e pluribus unum? *Mol Microbiol* 68:827–837. <https://doi.org/10.1111/j.1365-2958.2008.06197.x>.
- Averhoff B, Friedrich A. 2003. Type IV pili-related natural transformation systems: DNA transport in mesophilic and thermophilic bacteria. *Arch Microbiol* 180:385–393. <https://doi.org/10.1007/s00203-003-0616-6>.
- Bradley DE. 1980. A function of *Pseudomonas aeruginosa* PAO polar pili: twitching motility. *Can J Microbiol* 26:146–154. <https://doi.org/10.1139/m80-022>.
- Burrows LL. 2005. Weapons of mass retraction. *Mol Microbiol* 57:878–888. <https://doi.org/10.1111/j.1365-2958.2005.04703.x>.
- Mattick JS. 2002. Type IV pili and twitching motility. *Annu Rev Microbiol* 56:289–314. <https://doi.org/10.1146/annurev.micro.56.012302.160938>.
- Chang YW, Rettberg LA, Treuner-Lange A, Iwasa J, Sogaard-Andersen L, Jensen GJ. 2016. Architecture of the type IVa pilus machine. *Science* 351:aad2001. <https://doi.org/10.1126/science.aad2001>.
- Siewering K, Jain S, Friedrich C, Webber-Birungi MT, Semchonok DA, Binzen I, Wagner A, Huntley S, Kahnt J, Klingl A, Boekema EJ, Sogaard-Andersen L, van der Does C. 2014. Peptidoglycan-binding protein TsaP functions in surface assembly of type IV pili. *Proc Natl Acad Sci U S A* 111:E953–E961. <https://doi.org/10.1073/pnas.1322889111>.
- Coil DA, Anne J. 2010. The role of *fimV* and the importance of its tandem repeat copy number in twitching motility, pigment production, and morphology in *Legionella pneumophila*. *Arch Microbiol* 192:625–631. <https://doi.org/10.1007/s00203-010-0590-8>.
- Semmler AB, Whitchurch CB, Leech AJ, Mattick JS. 2000. Identification of a novel gene, *fimV*, involved in twitching motility in *Pseudomonas aeruginosa*. *Microbiology* 146(Pt 6):1321–1332. <https://doi.org/10.1099/00221287-146-6-1321>.
- Oldfield NJ, Bland SJ, Taraktsoglou M, Dos Ramos FJ, Robinson K, Wooldridge KG, Ala'Aldeen DA. 2007. T-cell stimulating protein A (TspA) of *Neisseria meningitidis* is required for optimal adhesion to human cells. *Cell Microbiol* 9:463–478. <https://doi.org/10.1111/j.1462-5822.2006.00803.x>.
- Bertrand JJ, West JT, Engel JN. 2010. Genetic analysis of the regulation of type IV pilus function by the Chp chemosensory system of *Pseudomonas aeruginosa*. *J Bacteriol* 192:994–1010. <https://doi.org/10.1128/JB.01390-09>.
- Whitchurch CB, Leech AJ, Young MD, Kennedy D, Sargent JL, Bertrand JJ, Semmler AB, Mellick AS, Martin PR, Alm RA, Hobbs M, Beatson SA, Huang B, Nguyen L, Commolli JC, Engel JN, Darzins A, Mattick JS. 2004. Characterization of a complex chemosensory signal transduction system which controls twitching motility in *Pseudomonas aeruginosa*. *Mol Microbiol* 52:873–893. <https://doi.org/10.1111/j.1365-2958.2004.04026.x>.
- Darzins A. 1994. Characterization of a *Pseudomonas aeruginosa* gene cluster involved in pilus biosynthesis and twitching motility: sequence similarity to the chemotaxis proteins of enterics and the gliding bacterium *Myxococcus xanthus*. *Mol Microbiol* 11:137–153. <https://doi.org/10.1111/j.1365-2958.1994.tb00296.x>.
- Sourjik V, Schmitt R. 1998. Phosphotransfer between CheA, CheY1, and CheY2 in the chemotaxis signal transduction chain of *Rhizobium meliloti*. *Biochemistry* 37:2327–2335. <https://doi.org/10.1021/bi972330a>.
- Darzins A. 1993. The *pilG* gene product, required for *Pseudomonas aeruginosa* pilus production and twitching motility, is homologous to the enteric, single-domain response regulator CheY. *J Bacteriol* 175:5934–5944. <https://doi.org/10.1128/jb.175.18.5934-5944.1993>.
- Fulcher NB, Holliday PM, Klem E, Cann MJ, Wolfgang MC. 2010. The *Pseudomonas aeruginosa* Chp chemosensory system regulates intracellular cAMP levels by modulating adenylate cyclase activity. *Mol Microbiol* 76:889–904. <https://doi.org/10.1111/j.1365-2958.2010.07135.x>.
- Silversmith RE, Wang B, Fulcher NB, Wolfgang MC, Bourret RB. 2016. Phosphoryl group flow within the *Pseudomonas aeruginosa* Pil-Chp chemosensory system: differential function of the eight phosphotransferase and three receiver domains. *J Biol Chem* 291:17677–17691. <https://doi.org/10.1074/jbc.M116.737528>.
- Luo Y, Zhao K, Baker AE, Kuchma SL, Coggan KA, Wolfgang MC, Wong GC, O'Toole GA. 2015. A hierarchical cascade of second messengers regulates *Pseudomonas aeruginosa* surface behaviors. *mBio* 6:e02456-14. <https://doi.org/10.1128/mBio.02456-14>.
- Persat A, Inclan YF, Engel JN, Stone HA, Gitai Z. 2015. Type IV pili mechanistically regulate virulence factors in *Pseudomonas aeruginosa*. *Proc Natl Acad Sci U S A* 112:7563–7568. <https://doi.org/10.1073/pnas.1502025112>.
- Wolfgang MC, Lee VT, Gilmore ME, Lory S. 2003. Coordinate regulation of bacterial virulence genes by a novel adenylate cyclase-dependent signaling pathway. *Dev Cell* 4:253–263. [https://doi.org/10.1016/S1534-5807\(03\)00019-4](https://doi.org/10.1016/S1534-5807(03)00019-4).
- Inclan YF, Persat A, Greninger A, Von Dollen J, Johnson J, Krogan N, Gitai Z, Engel JN. 2016. A scaffold protein connects type IV pili with the Chp chemosensory system to mediate activation of virulence signaling in *Pseudomonas aeruginosa*. *Mol Microbiol* 101:590–605. <https://doi.org/10.1111/mmi.13410>.
- Buist G, Steen A, Kok J, Kuipers OP. 2008. LysM, a widely distributed protein motif for binding to (peptido)glycans. *Mol Microbiol* 68:838–847. <https://doi.org/10.1111/j.1365-2958.2008.06211.x>.
- Blatch GL, Lasse M. 1999. The tetratricopeptide repeat: a structural motif mediating protein-protein interactions. *Bioessays* 21:932–939.
- Buensucseso RN, Nguyen Y, Zhang K, Daniel-Ivad M, Sugiman-Marangos SN, Fleetwood AD, Zhulin IB, Junop MS, Howell PL, Burrows LL. 2016. The conserved tetratricopeptide repeat-containing C-terminal domain of *Pseudomonas aeruginosa* FimV is required for its cyclic AMP-dependent and -independent functions. *J Bacteriol* 198:2263–2274. <https://doi.org/10.1128/JB.00322-16>.
- Coil DA, Vandersmissen L, Ginevra C, Jarraud S, Lammertyn E, Anne J. 2008. Intragenic tandem repeat variation between *Legionella pneumophila* strains. *BMC Microbiol* 8:218. <https://doi.org/10.1186/1471-2180-8-218>.
- Rossmann F, Brenzinger S, Knauer C, Dorrich AK, Bubendorfer S, Ruppert U, Bange G, Thormann KM. 2015. The role of FlhF and HubP as polar landmark proteins in *Shewanella putrefaciens* CN-32. *Mol Microbiol* 98:727–742. <https://doi.org/10.1111/mmi.13152>.
- Yamaichi Y, Bruckner R, Ringgaard S, Moll A, Cameron DE, Briegel A, Jensen GJ, Davis BM, Waldor MK. 2012. A multidomain hub anchors the chromosome segregation and chemotactic machinery to the bacterial pole. *Genes Dev* 26:2348–2360. <https://doi.org/10.1101/gad.199869.112>.
- Wehbi H, Portillo E, Harvey H, Shimkoff AE, Scheurwater EM, Howell PL, Burrows LL. 2011. The peptidoglycan-binding protein FimV promotes assembly of the *Pseudomonas aeruginosa* type IV pilus secretin. *J Bacteriol* 193:540–550. <https://doi.org/10.1128/JB.01048-10>.
- Carter T, Buensucseso RN, Tammam S, Lamers RP, Harvey H, Howell PL, Burrows LL. 2017. The type IVa pilus machinery is recruited to sites of future cell division. *mBio* 8:e02103-16. <https://doi.org/10.1128/mBio.02103-16>.
- Jansari VH, Potharla VY, Riddell GT, Bardy SL. 2016. Twitching motility and cAMP levels: signal transduction through a single methyl-accepting chemotaxis protein. *FEMS Microbiol Lett* 363:fnw119. <https://doi.org/10.1093/femsle/fnw119>.
- Fuchs EL, Brutinel ED, Jones AK, Fulcher NB, Urbanowski ML, Yahr TL, Wolfgang MC. 2010. The *Pseudomonas aeruginosa* Vfr regulator controls global virulence factor expression through cyclic AMP-dependent and -independent mechanisms. *J Bacteriol* 192:3553–3564. <https://doi.org/10.1128/JB.00363-10>.
- Inclan YF, Huseby MJ, Engel JN. 2011. FimL regulates cAMP synthesis in *Pseudomonas aeruginosa*. *PLoS One* 6:e15867. <https://doi.org/10.1371/journal.pone.0015867>.
- Nolan LM, Beatson SA, Croft L, Jones PM, George AM, Mattick JS, Turnbull L, Whitchurch CB. 2012. Extragenic suppressor mutations that restore twitching motility to *fimL* mutants of *Pseudomonas aeruginosa*

- are associated with elevated intracellular cyclic AMP levels. *Microbiologyopen* 1:490–501. <https://doi.org/10.1002/mbo3.49>.
35. Whitchurch CB, Beatson SA, Comolli JC, Jakobsen T, Sargent JL, Bertrand JJ, West J, Klausen M, Waite LL, Kang PJ, Tolker-Nielsen T, Mattick JS, Engel JN. 2005. *Pseudomonas aeruginosa* *fimL* regulates multiple virulence functions by intersecting with Vfr-modulated pathways. *Mol Microbiol* 55:1357–1378. <https://doi.org/10.1111/j.1365-2958.2005.04479.x>.
 36. Topal H, Fulcher NB, Bitterman J, Salazar E, Buck J, Levin LR, Cann MJ, Wolfgang MC, Steegborn C. 2012. Crystal structure and regulation mechanisms of the CyaB adenylyl cyclase from the human pathogen *Pseudomonas aeruginosa*. *J Mol Biol* 416:271–286. <https://doi.org/10.1016/j.jmb.2011.12.045>.
 37. Boyd JM. 2000. Localization of the histidine kinase PilS to the poles of *Pseudomonas aeruginosa* and identification of a localization domain. *Mol Microbiol* 36:153–162. <https://doi.org/10.1046/j.1365-2958.2000.01836.x>.
 38. Boyd JM, Koga T, Lory S. 1994. Identification and characterization of PilS, an essential regulator of pilin expression in *Pseudomonas aeruginosa*. *Mol Gen Genet* 243:565–574. <https://doi.org/10.1007/BF00284205>.
 39. Kilmury SL, Burrows LL. 2016. Type IV pilins regulate their own expression via direct intramembrane interactions with the sensor kinase PilS. *Proc Natl Acad Sci U S A* 113:6017–6022. <https://doi.org/10.1073/pnas.1512947113>.
 40. Kearns DB. 2010. A field guide to bacterial swarming motility. *Nat Rev Microbiol* 8:634–644. <https://doi.org/10.1038/nrmicro2405>.
 41. Bulyha I, Schmidt C, Lenz P, Jakovljevic V, Hone A, Maier B, Hoppert M, Sogaard-Andersen L. 2009. Regulation of the type IV pili molecular machine by dynamic localization of two motor proteins. *Mol Microbiol* 74:691–706. <https://doi.org/10.1111/j.1365-2958.2009.06891.x>.
 42. Bren A, Eisenbach M. 1998. The N terminus of the flagellar switch protein, FlIM, is the binding domain for the chemotactic response regulator, CheY. *J Mol Biol* 278:507–514. <https://doi.org/10.1006/jmbi.1998.1730>.
 43. Mancl JM, Black WP, Robinson H, Yang Z, Schubot FD. 2016. Crystal structure of a type IV pilus assembly ATPase: insights into the molecular mechanism of PilB from *Thermus thermophilus*. *Structure* 24:1886–1897. <https://doi.org/10.1016/j.str.2016.08.010>.
 44. Tsai CL, Tainer JA. 2016. The ATPase motor turns for type IV pilus assembly. *Structure* 24:1857–1859. <https://doi.org/10.1016/j.str.2016.10.002>.
 45. McCallum M, Tammam S, Khan A, Burrows LL, Howell PL. 2017. The molecular mechanism of the type IVa pilus motors. *Nat Commun* 8:15091. <https://doi.org/10.1038/ncomms15091>.
 46. Murray TS, Kazmierczak BI. 2006. FlhF is required for swimming and swarming in *Pseudomonas aeruginosa*. *J Bacteriol* 188:6995–7004. <https://doi.org/10.1128/JB.00790-06>.
 47. Ethier J, Boyd JM. 2000. Topological analysis and role of the transmembrane domain in polar targeting of PilS, a *Pseudomonas aeruginosa* sensor kinase. *Mol Microbiol* 38:891–903. <https://doi.org/10.1046/j.1365-2958.2000.02189.x>.
 48. Ayers M, Sampaleanu LM, Tammam S, Koo J, Harvey H, Howell PL, Burrows LL. 2009. PilM/N/O/P proteins form an inner membrane complex that affects the stability of the *Pseudomonas aeruginosa* type IV pilus secretin. *J Mol Biol* 394:128–142. <https://doi.org/10.1016/j.jmb.2009.09.034>.
 49. Kus JV, Tullis E, Cvitkovitch DG, Burrows LL. 2004. Significant differences in type IV pilin allele distribution among *Pseudomonas aeruginosa* isolates from cystic fibrosis (CF) versus non-CF patients. *Microbiology* 150:1315–1326. <https://doi.org/10.1099/mic.0.26822-0>.
 50. Schneider CA, Rasband WS, Eliceiri KW. 2012. NIH Image to ImageJ: 25 years of image analysis. *Nat Methods* 9:671–675. <https://doi.org/10.1038/nmeth.2089>.
 51. Ducret A, Quardokus EM, Brun YV. 2016. Microbel, a tool for high throughput bacterial cell detection and quantitative analysis. *Nat Microbiol* 1:16077. <https://doi.org/10.1038/nmicrobiol.2016.77>.
 52. Köhler T, Curty LK, Barja F, van Delden C, Pechere JC. 2000. Swarming of *Pseudomonas aeruginosa* is dependent on cell-to-cell signaling and requires flagella and pili. *J Bacteriol* 182:5990–5996. <https://doi.org/10.1128/JB.182.21.5990-5996.2000>.
 53. Watson AA, Mattick JS, Alm RA. 1996. Functional expression of heterologous type 4 fimbriae in *Pseudomonas aeruginosa*. *Gene* 175:143–150. [https://doi.org/10.1016/0378-1119\(96\)00140-0](https://doi.org/10.1016/0378-1119(96)00140-0).
 54. Simon V, Schumann W. 1987. In vivo formation of gene fusions in *Pseudomonas putida* and construction of versatile broad-host-range vectors for direct subcloning of Mu d1 and Mu d2 fusions. *Appl Environ Microbiol* 53:1649–1654.
 55. Asikyan ML, Kus JV, Burrows LL. 2008. Novel proteins that modulate type IV pilus retraction dynamics in *Pseudomonas aeruginosa*. *J Bacteriol* 190:7022–7034. <https://doi.org/10.1128/JB.00938-08>.